Dynamics and polarization of group-III nitride lattices: A first-principles study

F. Bechstedt, Ulrike Grossner, and J. Furthmüller
Institut für Festkörpertheorie und Theoretische Optik Friedrich-Schiller-Universität, Max-Wien-Platz 1, D-07743 Jena, Germany
(Received 10 May 1999; revised manuscript received 20 September 1999)

We present a comprehensive picture of dynamical and electrostatic properties of boron, aluminum, gallium, and indium nitride. Our investigations are based on *first-principles* calculations within the density-functional theory and the local-density approximation. Starting from a careful investigation of the structure of the wurtzite and zinc-blende polytypes, important properties of the nitride lattices are studied. Among them are the dynamical charges and the spontaneous polarization field. The phonon dispersion relations are presented for the four group-III nitrides. Chemical trends are derived and related to the different strengths of covalent and ionic bonding.

I. INTRODUCTION

Among the III-V semiconductors the group-III nitrides have attracted both scientific and technological interest in recent years. The nitrides AlN, GaN, and InN are regarded as promising wide-band-gap semiconductors for optoelectronic applications in the short-wavelength range as well as for high-temperature, high-power, and high-frequency electronic devices. The fascinating mechanical and thermal properties of BN crystallizing in a zinc-blende structure, such as hardness, high melting point, high thermal conductivity, and large elastic moduli, make it useful for protective coatings. The outstanding properties of the nitrides are mainly related to the specific role of the nitrogen atoms. The smallness of the N atoms gives rise to the formation of short bonds[1] with a large bond ionicity.[2]

At ambient conditions, BN crystallizes usually in hexagonal graphitelike structures with a two-bilayer stacking sequence. The denser zinc-blende and wurtzite phases of BN are thermodynamically stable at high pressure and high temperature.[3] The number of bilayers of cations and anions parallel to the cubic [111] or hexagonal [0001] direction varies from 3 to 2. Consequently, the cubic (hexagonal) zinc-blende (wurtzite) structure is denoted by $3C$ $(2H)$. The more ionic compounds AlN, GaN, and InN crystallize in the wurtzite structure at ambient conditions.[4] However, several papers report the occurrence of the metastable $3C$ polytype of AlN.[5] Also thin films of AlN, GaN, and InN with zinc-blende structure have been grown epitaxially.[6–8]

Considerable progress of the theoretical description of the bulk nitrides has been achieved in recent years. In particular, *ab initio* density-functional theory (DFT) calculations in the framework of the local-density approximation (LDA) have contributed to a reasonable picture of the structural, electronic, vibronic, and elastic properties.[9–19] Unfortunately, a fully consistent picture is still lacking. For example, despite several years of theoretical research, there are no *ab initio* calculations of the lattice vibrations in InN. The mechanism and the most important contributions to the spontaneous polarization in wurtzite nitrides are not fully understood.

In this paper, we present results for the static and vibrating lattices of the group-III nitrides BN, AlN, GaN, and InN. The used non-normconserving pseudopotentials are softened according to new rules recently formulated.[20] They are important for the reduction of the numerical effort due to the lack of p electrons in the N and B cores and, in particular, the treatment of the Ga $3d$ and In $4d$ electrons as valence electrons. For both the wurtzite and zinc-blende phases structural, dynamical, and electrostatic properties are considered. Chemical trends are studied in detail.

II. COMPUTATIONAL METHOD

Our calculations are based on the DFT-LDA.[21] Besides the valence electrons also the semicore Ga $3d$ and In $4d$ states are explicitly considered. Their interaction with the atomic cores is treated by non-normconserving *ab initio* Vanderbilt pseudopotentials.[22] They allow a substantial potential softening also for first-row elements with the lack of core p electrons as well as for the attraction of shallow d electrons.[20] As a consequence of the optimization the plane-wave expansion of the single-particle eigenfunctions may be restricted by an energy cutoff of 22.1 (BN), 14.4 (AlN), 16.2 (GaN), and 15.5 Ry (InN). The cutoffs have been carefully tested and successfully applied to the properties of bulk zinc-blende nitrides and their cleavage surfaces.[23] In the BN case slightly harder pseudopotentials are used in order to avoid an unphysical strong overlap of wave functions due to the small lattice constant. The many-body electron-electron interaction is described by the Ceperley-Alder functional as parametrized by Perdew and Zunger.[24] The **k**-space integrals are approximated by sums over 10 (zinc-blende) or 12 (wurtzite) special points of the Chadi-Cohen type[25] within the irreducible part of the Brillouin zone (BZ). Our calculations employ the conjugate-gradient method to minimize the total energy. Explicitly we use the Vienna *ab initio* simulation package.[26,27]

III. RESULTS AND DISCUSSION

A. Structural properties

The ground-state properties in the pressure-free case are obtained considering the minimum of the total energy with respect to the cell volume. Whereas in the zinc-blende case the volume is directly related to the cubic lattice constant a_0, for wurtzite the volume is determined by the two lattice con-

 ©2000 The American Physical Society

TABLE I. Structural parameters of zinc-blende and wurtzite group-III nitrides. Other calculated values (Refs. 10 and 12) and experimental data (second value, taken from the data collections in Refs. 10 and 12) are given in parentheses.

Parameter	BN	AlN	GaN	InN
a_0 (Å)	3.60	4.34	4.46	4.97
	(3.58, 3.615)	(4.34, 4.38)	(4.46, 4.5)	(4.93, 4.98)
B_0 (Mbar)	4.01	2.09	1.83	1.33
	(3.52, 3.69–4.65)	(2.07, 2.02)	(1.87, 1.90)	(1.40, 1.37)
a (Å)	2.52	3.08	3.15	3.53
	(2.508, 2.55)	(3.08, 3.110)	(3.16, 3.190)	(3.50, 3.544)
c/a	1.655	1.607	1.631	1.632
	(1.666, 1.648)	(1.604, 1.601)	(1.626, 1.627)	(1.619, 1.613)
u	0.3741	0.3824	0.3815	0.3780
	(0.3713,)	(0.3814, 0.3821)	(0.3770, 0.3770)	(0.3784,)
B (Mbar)	3.91	2.03	1.95	1.25
	(4.12,)	(2.05, 2.02)	(2.02, 1.95)	(1.39, 1.26)

stants a and c. However, there is a third structural degree of freedom u that characterizes the relative length of the group-III N bonds parallel to the c axis. The equilibrium volume and the isothermal bulk modulus at zero pressure, B, follow from a fit of the total energy as a function of volume to the Murnaghan equation of state.[28] The two other independent structural parameters c/a and u are obtained from a polynomial fit of the total energy.

The calculated values are listed in Table I. They are compared with results of other converged plane-wave calculations using normconserving pseudopotentials of the Bachelet-Hamann-Schlüter type[10,12] as well as experimental data taken from the corresponding collections in Refs. 10 and 12. We observe an excellent agreement with previous theoretical values. This holds in particular for AlN and GaN. However, this good agreement can be also stated in the case of comparison with the experimental data. Overall, the lattice constants are only about 1% smaller than the measured values. Such derivations are typical for well-converged DFT-LDA calculations. The discrepancies are even smaller in the zinc-blende case. Somewhat surprising is the excellent reproduction of the bulk moduli by the theory, in particular in the wurtzite case. The lattice constants and bulk moduli follow clear chemical trends with the size of the group-III atoms.

These clear chemical trends are somewhat in contrast to the dependencies of internal structural parameters u and the ratio c/a of the unit cell of the hexagonal phases. For GaN and InN the ratios c/a approach the ideal value $c/a=1.633$. The relative length u of the group-III N bond parallel to the c axis is close to its ideal value $u=0.375$ only in the BN case where the favorable structure corresponds to zinc blende. For the more ionic compounds the u values are larger, but decrease more or less with rising bond ionicity. The corresponding values obtained as the charge-asymmetry coefficients g from *ab initio* electron density distributions are $g=0.484$ (BN), 0.794 (AlN), 0.780 (GaN), and 0.853 (InN).[2]

B. Dielectric and lattice-dynamical properties

The dielectric and lattice-dynamical properties can be calculated using a combination of DFT and generalized response theory, the density-functional perturbation theory (DFPT).[29] Effective ion charges and phonon dispersion relations have been calculated by Karch and co-workers[16,18] for BN, AlN, and GaN using this theory. However, these authors were unable to describe reasonably the lattice-dynamical properties of InN using the same type of normconserving pseudopotentials. On the other hand, it is complicated to combine DFPT with non-normconserving pseudopotentials.[30] However, such a combination is possible in the framework of a generalization of the *ab initio* force constant method.[31] The success is shown in a recent paper for BN. We follow the line of Refs. 31–33 in calculating directly the interatomic force constant matrix. In the zinc-blende case we consider a $2\times2\times2$ supercell containing 64 atoms. The displacement of a single atom in the supercell induces forces acting on the surrounding atoms, which are calculated via the Hellmann-Feynman theorem. According to the folding arguments one ends up with force constants at several high-symmetry $\mathbf{k}$ points in the Brillouin zone of the zinc-blende structure. In order to obtain complete dispersion relations along high-symmetry directions the force-constant matrix is interpolated.

The method is rather similar to the frozen-phonon method. It therefore describes the LO modes incorrectly. The long-range electric field is not included. Kern *et al.*[31] suggested to determine this field or, more strictly speaking, the screened Born ion charges that generate this field, from an artifact of the periodic boundary conditions. The false electrostatic field occurring in the supercell approach should be compensated to describe the reality. This allows the determination of the screened Born charges $Z^*=Z_B/\sqrt{\varepsilon_\infty}$ that differ only in sign between cation and anion. Using these charges the nonanalytical long-range electric part of the dynamical matrix[34] is constructed and added to the force constant matrix.[31] It is diagonalized and the resulting eigenvalues are used to compute the phonon density of states by means of the linear-tetrahedron method and a 45^3 grid in the BZ.

The phonon frequencies resulting for the high-symmetry points Γ, X, and L in the fcc BZ are listed in Table II. Complete dispersion relations are presented in Fig. 1. In the case of BN, AlN, and GaN we compare our data in Table II with other first-principles calculations using the DFPT (Refs.

TABLE II. Phonon frequencies calculated at the high-symmetry points Γ, X, L, K, and W for the zinc-blende polytype of BN, AlN, GaN, and InN. In the cases of K and W the two splitted TO values are given. Frequencies from DFPT (Refs. 16 and 18) (first value) and experimental data (second value) are in parentheses. All values are given in units of cm^{-1}.

Mode	BN	AlN	GaN	InN
Γ_{TO}	1061 (1040, 1055[a])	665 (662, 655[b])	567 (560, 552,[c] 552,[d] 555[e])	467 (457[f])
Γ_{LO}	1280 (1285, 1305[a])	890 (907, 902[b])	746 (750, 743,[c] 737,[d] 741[e])	596 (588[f])
X_{TA}	706 (707)	341 (340)	197 (195)	116
X_{LA}	1018 (1026)	588 (590)	351 (353)	231
X_{TO}	939 (902)	668 (674)	623 (628)	518
X_{LO}	1154 (1152)	716 (734)	695 (709)	567
L_{TA}	487 (489)	226 (230)	138 (139)	78
L_{LA}	982 (980)	585 (582)	349 (345)	227
L_{TO}	1009 (981)	655 (656)	587 (585)	488
L_{LO}	1149 (1142)	735 (750)	708 (720)	573
K_{TA}	675	320	187	108
	877	436	254	155
K_{LA}	904	534	321	212
K_{TO}	930	652	610	543
	987	671	654	506
K_{LO}	1092	729	695	563
W_{TA}	803	381	218	131
	816	427	251	151
W_{LA}	886	509	308	204
W_{TO}	982	658	636	527
	1009	677	646	541
W_{LO}	1022	726	692	557

[a]Doll (Ref. 35).
[b]Harima *et al.* (Ref. 36).
[c]H. Siegle *et al.* (Ref. 37).
[d]Harima *et al.* (Ref. 6).
[e]Tabata *et al.* (Ref. 38).
[f]Tabata *et al.* (Ref. 41).

16 and 18) and first-order Raman data for cubic epitaxial layers.[6,35–38] The agreement of the two different *ab initio* calculations for the acoustic phonon branches is excellent. The maximum deviation amounts to 4 cm^{-1}. The deviations in the frequency region of the optical branches are slightly larger. The main reason is related to the smaller screened effective ion charges Z^* in the present calculations. We underestimate the zone-center LO-TO splittings by 21, 20, and 11 cm^{-1} for BN, AlN, and GaN. The agreement of the frequencies calculated for Γ phonons and the first-order Raman data measured for cubic epitaxial layers is also satisfactory (cf. Table II). The discrepancy in the case of the TO phonons is a result of the overestimation of the corresponding force constants due to the LDA underestimation of the lattice constant.

The short-range contribution f to the interatomic force constants follows the relation[39]

$$f=[2\omega_{TO}^2(\Gamma)+\omega_{LO}^2(\Gamma)]/3\mu, \tag{1}$$

where μ is the reduced mass. A fit to the four nitrides under consideration gives the dependence $f=38.74\times10^{-9}$ N/m/$(a_0/\text{Å})^{2.7}$ on the lattice constant. This dependence is somewhat weaker than predicted for covalent materials in the framework of the bond orbital model.[1] We trace this fact back to the strong ionic character of the bonding in the nitrides. The observed length dependence of the force constant indicates that the underestimation of the lattice constant by 1% gives rise to an increase of the optical phonon frequency by 1.4%.

The splitting of the LO and TO phonon modes at Γ is governed by the accompanying macroscopic electric field. The corresponding screened charges of the ions are given by[40]

$$Z^*=\left\{\frac{\Omega_0\mu}{4\pi e^2}[\omega_{LO}^2(\Gamma)-\omega_{TO}^2(\Gamma)]\right\}^{1/2} \tag{2}$$

with the unit cell volume Ω_0. From the fit procedure we estimate $Z^*=0.86$, 1.16, 1.11, and 1.03 for BN, AlN, GaN, and InN, respectively. These values are smaller than those calculated within the DFPT, $Z^*=0.91$, 1.21, and 1.14 for BN, AlN, and GaN.[16,18] The fit procedure contains a general tendency for an underestimation of the charges in comparison to the direct calculation. The nonmonotonous behavior with respect to the static bond ionicity g may be related to the Born effective charge, e.g., within the simplifying bond-

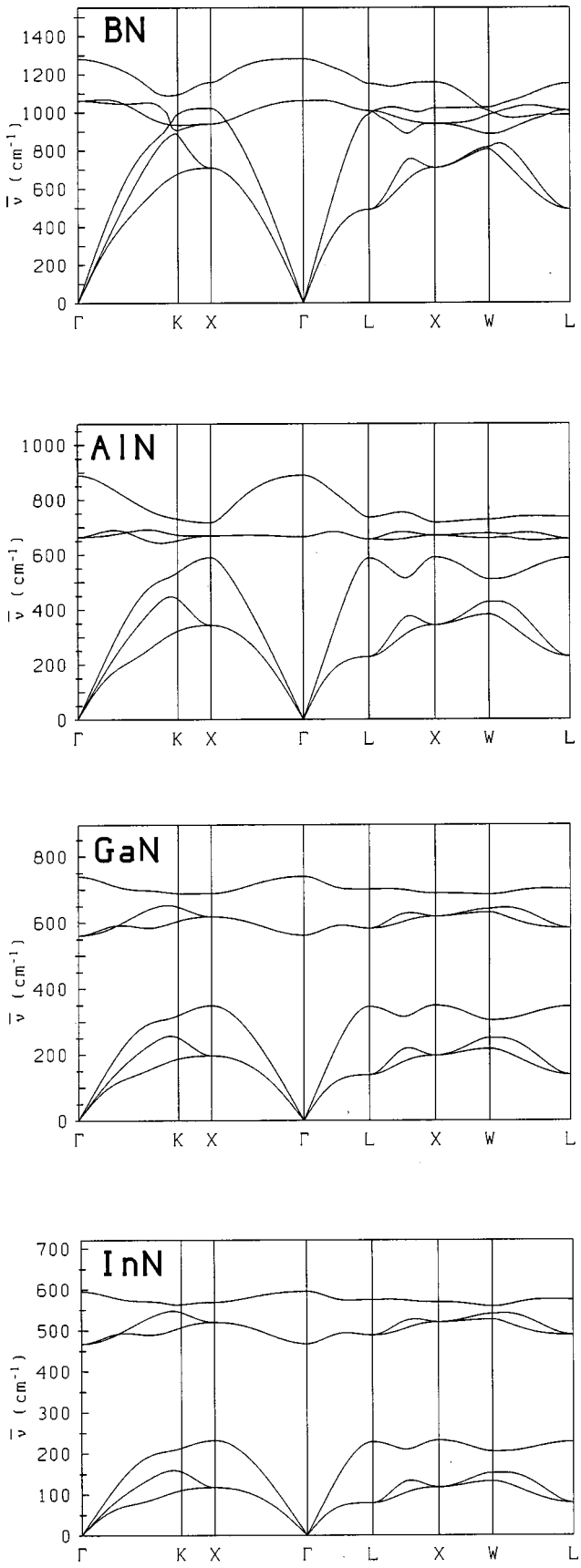

FIG. 1. Calculated phonon dispersion curves of the zinc-blende nitrides.

orbital picture $Z_B = 4g - 1 + \frac{8}{3}g(1-g)$, and the dependence of the dielectric constant $\varepsilon_\infty - 1 \approx (1-g^2)$.[1] Whereas the picture of the Raman modes of BN, AlN, and GaN is rather complete (cf., e.g., Refs. 16 and 18), this is not the case for InN. The agreement between theory and experiment[41] is satisfying. The overestimation of the theoretical values corresponds nearly to the value that we have estimated because of the underestimation of the lattice constant within DFT-LDA. Other calculations using the linear muffin-tin orbital (LMTO) and frozen-phonon method[13] completely fail with TO(Γ) frequencies of 540 cm^{-1}.

Our calculations can help to clarify the contradicting picture of the Raman modes for hexagonal InN, in particular considering the fact that the L point in the fcc BZ is folded onto the Γ point in the BZ of the $2H$ crystal. Consequently the LO(L) and LA(L) can be identified as the upper and lower B_1 modes and, respectively, TO(L) and TA(L) as the upper and lower E_2 modes. The corresponding values are also listed in Table II. That means, our *ab initio* theory predicts a frequency of about 488 (78) cm^{-1} for the higher (lower) E_2 modes in $2H$ InN. According to the relations between the zone-center optical phonons in $3C$ and $2H$ crystals of BN, AlN, and GaN (Refs. 16 and 18) also the frequencies of the E_1 and A_1 modes of wurtzite InN may be estimated. Assuming that the splittings of the TO(Γ) and LO(Γ) modes into the E_1 and A_1 phonons of the wurtzite structure are more or less the same in GaN and InN, we find 449 cm^{-1} [A_1(TO)], 475 cm^{-1} [E_1(TO)], 594 cm^{-1} [A_1(LO)], and 603 cm^{-1} [E_1(LO)]. These values are in close agreement with measured frequencies, although the interpretation of the measurements becomes complicated due to the nearly energetical overlap of the upper E_2 and A_1(TO) modes.[42] The values 590 (596) and 491 (495) cm^{-1} (Refs. 42 and 43) for the A_1(LO) and the E_2 phonon measured for $2H$-InN films do practically not differ from the theoretical ones. However, also the values 574 [A_1(LO)], 488 (E_2), 475 [E_1(TO)], and 446 cm^{-1} [A_1(TO)] (Ref. 44) measured for nearly polycrystalline wurtzite InN approach the frequencies estimated above. Measurements of four optical phonons at 190 (donated as lower E_2), 400 [donated as A_1(TO)], 490 [donated as E_1(TO)], and 590 cm^{-1} (donated as upper E_2) (Ref. 45) complete the picture. In the light of our calculations the highest modes have to be identified as E_2 and A_1(LO) modes, whereas the physical origin of the two lower modes remains unclear. Interpolation of the $In_{1-x}Ga_xN$ alloy reflectance data gives a TO-like phonon energy of about 478 cm^{-1},[46] which seems to be reasonable. However, the extrapolation of the TO data to the LO phonon branch by the authors completely fails with a LO-like phonon frequency of about 694 cm^{-1}. Altogether, we find also good agreement for the zone-center phonons with results of very recent Raman measurements.[47] The measured values are 593 [E_1(LO)], 586 [A_1(LO)], 488 (higher E_2), 475 [E_1(TO)], 447 [A_1(TO)], and 87 cm^{-1} (lower E_2).

The phonon dispersion relations given in Fig. 1 allow the extraction of the sound velocities in the nitrides. We do this only for the phonon propagation in the ΓX direction. Along this direction we have calculated the dynamical matrix exactly at three **k** points. For that reason the interpolation procedure should be of minor influence. For the transverse

TABLE III. Calculated elastic constants (in GPa) for cubic nitrides. In the case of BN measured values are also given (Ref. 48).

Constant	Ref.	BN	AlN	GaN	InN
c_{11}	Present	853	314	297	185
	13	837	298	282	182
	16	812	294		
	17		304	293	187
	Expt.	820			
c_{12}	Present	175	157	126	107
	13	182	164	159	125
	16	182	160		
	17		160	159	125
	Expt.	190			
c_{44}	Present	497	200	154	80
	13	493	187	142	79
	16	464	189		
	17		193	155	86
	Expt.	480			

phonons we find the velocities $v_t = 11.86$, 7.76, 4.96, and 3.38×10^3 ms^{-1} for BN, AlN, GaN, and InN, respectively. In the longitudinal case it follows that $v_l = 15.54$, 9.7, 6.88, and 5.16×10^3 ms^{-1} irrespectively. The sound velocities for the propagation along [100] allows the direct determination of the elastic stiffness constants c_{11} and c_{44}. The third independent elastic constant c_{12} is derived from the relation $B = (c_{11} + 2c_{12})/3$[1] and the bulk moduli in Table I. The results are summarized in Table III and compared with other theoretical results. Considering the different DFT-LDA methods and the different procedures for the calculations the agreement of the three groups of theoretical results is excellent. This holds also for the comparison with experimental data[48] available only for zinc-blende BN. Consequently, we conclude that the phonon dispersion relations in the frequency region of the acoustic phonons are reasonably described by the used *ab initio* force-constant method.

Figure 2 shows the phonon density of states (DOS) of BN, AlN, GaN, and InN. One immediately finds the dependence of the frequency gap between the acoustical and optical phonon branches on the material. This effect can be quite easily explained within the classical two-atomic linear chain where the frequency gap is given by zone-boundary vibrations with the nitrogen mass (upper limit) or the group-III atom mass (lower limit): the larger the mass difference between the two atoms the larger the frequency gap is. In the case of BN one can observe an overlap of the acoustical and optical phonon branches so that there is no visible gap in the DOS. This holds with the facts, that the boron mass is smaller than the nitrogen mass and the angular forces become more important than the electrostatic forces as a consequence of lower bond ionicity and larger covalent bonding. Other interesting features visible in the density of states are the remarkable changes of the dispersion of the optical branches. There is a strong reduction of the LO dispersion from the stronger bonded nitrides BN and AlN to GaN and InN. Also the dispersion of the TO phonon branches show a clear chemical trend accompanied by the inversion of the band dispersion. The strongest contributions to the density of the TO phonons arise from the Brillouin zone center. As a consequence of the nearly linear increase of the ratios $\omega_{TO}(\Gamma)/\omega_{TO}(X)$ and $\omega_{TO}(\Gamma)/\omega_{TO}(L)$ with decreasing cation mass, the frequencies of the zone-center TO phonons of BN (GaN, InN) are larger (smaller) than those of the zone-boundary phonons. In contrast, the TO phonon branch of AlN is nearly dispersionless, at least in the ΓX direction. Hence, the strongest contributions to the TO phonon density of states occur at the upper (lower) boundary for BN and AlN (GaN and InN). The comparison of the phonon densities of states of AlN, GaN, and InN with measured ones[47,49] indicates that the main features are fairly well reproduced. This holds for both the peak positions and the peak intensities. The experimental DOS have been derived from Raman measurements of ion-implanted samples.

C. Polarization fields

As materials with partially ionic bonds the group-III nitrides exhibit the piezoelectric effect. Piezoelectric polarization fields are induced for internal displacements of the group-III atoms relative to the nitrogen atoms in an elementary cell. In the zinc-blende case (T_d^2) this happens only for shear strains. For wurtzite crystals with lower symmetry (C_{6v}^4) piezoelectric polarization fields may be also induced by diagonal strains. However, even in the equilibrium the lower-symmetry wurtzite polytypes are expected to possess an intrinsic polarization field, since the four tetrahedral bonds around one atom are no longer equivalent, so that wurtzite crystals represent pyroelectrics. Meanwhile, the influence of such internal polarization fields has been observed via the quantum-confined Stark effect in optical spectra of layered nitride systems.[50,51]

The macroscopic polarization

$$\mathbf{P} = \frac{e}{\Omega_0} \int_{\Omega_0} d\mathbf{x}\mathbf{x} n(\mathbf{x}) \tag{3}$$

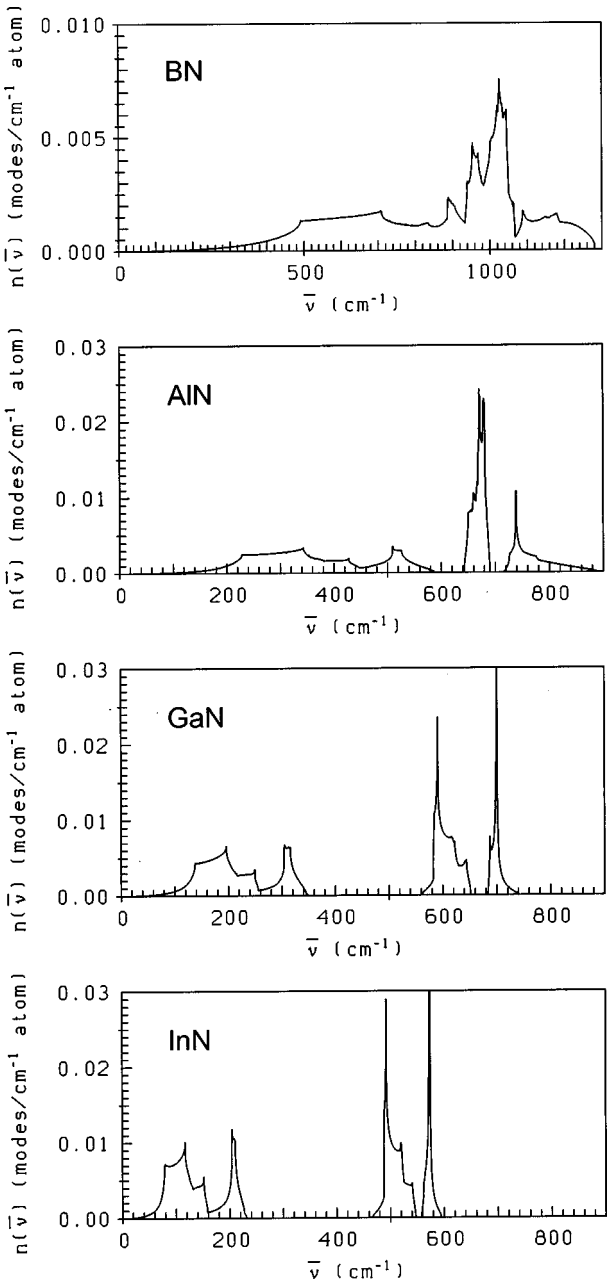

FIG. 2. Phonon density of states of the zinc-blende nitrides.

is related to the electron density $n(\mathbf{x})$ by definition as electric dipole moment per unit volume. Unfortunately, for an infinite crystal without center of inversion symmetry the polarization in Eq. (3) is an ill-defined quantity.[52] In order to eliminate the truncation and surface effects, we calculate this quantity in a supercell approach from *first principles* as the difference in the polarization $\Delta\mathbf{P}$ in a cubic reference material and in the wurtzite structure.[53] By definition the polarization field should vanish in a real cubic crystal. For symmetry reasons only the z component ΔP_z is nonzero. In explicit calculations[54–56] the spontaneous polarization in wurtzite SiC heterocrystalline structures with supercells consisting of both polytypes, $3C$ and $2H$, have been studied. The macroscopic polarization is related to a homogeneous electric field in each polytype region and, hence, to the gradient of the spatially averaged total one-electron potential

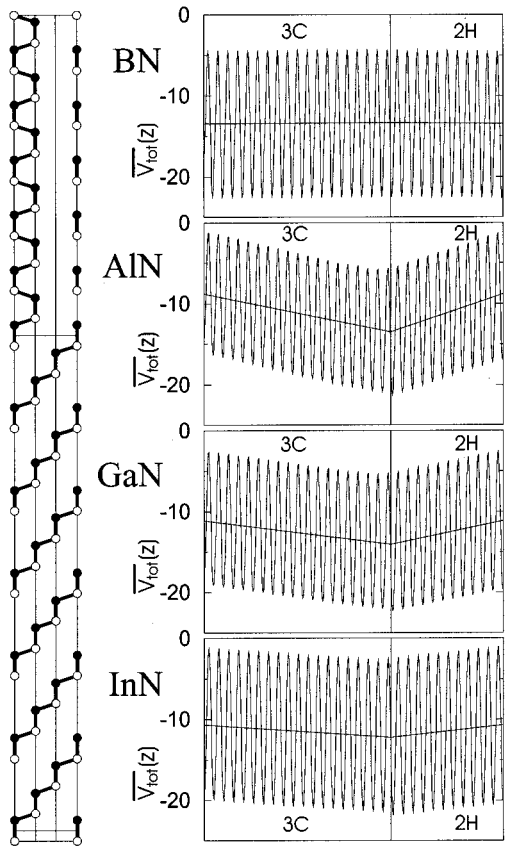

FIG. 3. Structure for a $(3C)_6(2H)_6$ cell and averaged total one-electron potentials. The vertical lines separate cubic and hexagonal stacking regions.

$$\Delta P_z = -\frac{1}{4\pi}\Delta E_z = -\frac{1}{4\pi}\left[\frac{d}{dz}\overline{V}_{\rm tot}(z)\bigg|_{2H} - \frac{d}{dz}\overline{V}_{tot}(z)\bigg|_{3C}\right]. \tag{4}$$

The total potential $V_{\rm tot}$ occurring in the Kohn-Sham equations of the DFT-LDA is averaged over the xy plane perpendicular to the c axis.

Explicitly we use supercells with 30 [111]- or [0001]-oriented group-III N bilayers.[55,56] In other words, $(3C)_6(2H)_6$ superlattices are studied. The lattice constants of the two polytypes differ in the plane perpendicular to the c axis. Since the result should be independent of the cubic reference system, we choose as the a-lattice constant of the 30H system that of the $2H$ structure. The c-lattice constant of the $30H$ supercell is then given as $(6c+18\sqrt{\frac{2}{3}}a)$ with c as the $2H$ lattice constant. The bonds parallel to the c axis are fixed in the $2H$ regions by the internal-cell parameter u, whereas these bond lengths in the $3C$ regions are given by $\sqrt{\frac{3}{8}}a$. The resulting macroscopic potentials $\overline{V}_{tot}(z)$ are plotted in Fig. 3. The derived spontaneous polarizations are listed in Table IV. The results are compared with those of another *ab initio* calculations, using the Berry phase approach to the polarization in solids,[57] and values calculated within the bond-orbital model.[1]

For comparison with results of other calculations[57] we have to stress that according to Eq. (4) only the macroscopic polarization measured in the presence of a depolarization

TABLE IV. Calculated spontaneous polarization P_z (in units of 10^{-3} C/m^2) for wurtzite group-III nitrides.

Ref.		BN	AlN	GaN	InN
Present	ΔP_z	≈ 0	-26	-14	-6
Present	P_z	≈ 0	-120	-74	-50
57	P_z		-81	-29	-32
Model	P_z	-32	-51	-50	-22

field $\overline{E}$ (Ref. 58) has been determined. Other authors call this polarization field the extrinsic one[54] or the longitudinal one.[53] In order to determine the macroscopic polarization P_z for the vanishing depolarization field,[58] the polarization induced in the electronic system by the electric fields present in the $2H$ and $3C$ regions have to be taken into account. This effect is proportional to the electronic susceptibility $(\overline{\varepsilon_\infty}-1)/4\pi$. For this intrinsic or transverse polarization field we therefore obtain

$$P_z=\overline{\varepsilon}_\infty \Delta P_z \tag{5}$$

with an effective electronic dielectric constant of the considered superlattice

$$\overline{\varepsilon}_\infty=\frac{(d_{2H}\varepsilon_\infty^{zz}+d_{3C}\varepsilon_\infty)}{(d_{2H}+d_{3C})}, \tag{6}$$

where the thicknesses d_{2H} and d_{3C} of the two polytype layers and the components parallel to the c axis of their dielectric tensors ε_∞^{zz} and ε_∞ have been introduced. From the *ab initio* calculations in Refs. 16, 18, and 58 we observe $\overline{\varepsilon_\infty}=4.59$ (BN), 4.52 (AlN), 5.41 (GaN), and 8.49 (InN). With these values the polarization fields at zero electric field follow. They are also given in Table IV.

Interpreting the charge-symmetry coefficients $g_\parallel$ and $g_\perp$ (Ref. 2) as the ionicities of the bonds parallel to the c axis or with an angle of about 70° to the c axis, one has to deal with the bond dipoles $\mathbf{p}_{\parallel/\perp}=e\mathbf{g}_{\parallel/\perp}\boldsymbol{\tau}_{\parallel/\perp}$. The vectors $\boldsymbol{\tau}_{\parallel/\perp}$ are nearly tetrahedron vectors. In hexagonal Cartesian coordinates it holds $\boldsymbol{\tau}_\parallel=uc(0,0,1)$ and, for example, $\boldsymbol{\tau}_\perp=[0,-a/\sqrt{3},(\frac{1}{2}-u)c]$. The summation over the eight bonds per $2H$ unit cell with the volume Ω_0 leads with Eq. (3) to the expression

$$P_z=-\frac{2ec}{\Omega_0}[4g_\perp(\tfrac{3}{8}-u)+(g_\perp-g_\parallel)u]. \tag{7}$$

There are two contributions to the spontaneous polarization field parallel to the c axis of $2H$. They are related directly or indirectly to the deformation of the bonding tetrahedra in the wurtzite structure. This is evident for the first contribution because $u=\frac{3}{8}$ defines an ideal tetrahedron. The second term is proportional to the different bond ionicities. The values $g_\parallel$ and $g_\perp$ are almost identical to those g of the zinc-blende structures. For AlN Karch and Bechstedt[16] found $g_\perp=g(1-0.0025)$ and $g_\parallel=g(1+0.259)$. Nevertheless, the term $(g_\perp-g_\parallel)$ is non-negligible, in particular for nitrides with u and c/a close to the ideal values $\frac{3}{8}$ or $\sqrt{\frac{3}{8}}$. This becomes obvious within the bond-orbital model. One derives

$$g_\perp-g_\parallel\approx\tfrac{1}{2}g(1-g^2)\left[\left(\frac{3}{u8}\right)^2-\frac{81}{64}\frac{1}{3a^2/c^2+u^2}\right]$$

in a linear approximation. We mention that expression (7) also defines the piezoelectric polarization field along the z axis if the wurtzite structure is strained with new structural parameters $\tilde{c}$, $\tilde{a}$, and $\tilde{u}$ different from the equilibrium values c, a, and u. In linear order with respect to diagonal components of the strain tensor, the polarization field is expressed by the piezoelectric coefficients $e_{33}=c(\partial P_z/\partial\tilde{c})_{\tilde{c}=c}$ and $e_{31}=a(\partial P_z/\partial\tilde{a})_{\tilde{a}=a}$.

The two *ab initio* calculations and our estimate in the framework of the bond-orbital model give rise to the same order of magnitude of the intrinsic polarization (cf. Table IV). The variation of the absolute numbers between the two first-principles calculations is mainly a consequence of the extreme accuracy of the structural optimization that is required for such calculations. For instance, the large deviations in the results for GaN may be related to the difference in the u parameters, $u=0.381$ (present) and $u=0.376$.[57] Similar large deviations are observed within *ab initio* calculations for wurtzite BeO, $P_z=-16\times10^{-3}$ C/m^2 (Ref. 57) and $P_z=-45\times10^{-3}$ C/m^2.[53] Because of the accuracy requirements for the atomic structure we are skeptical of the possibility of highly accurate calculations of the spontaneous polarization fields. The accuracy of the determination of the equilibrium atomic structure parameters within standard DFT-LDA calculations is perhaps not sufficient enough. This holds in particular for the determination of the internal-cell parameter u, but also for the ratio of the lattice constants c and a.

IV. SUMMARY

In conclusion, we have presented well-converged *ab initio* studies of the group-III nitrides crystallizing in zinc-blende and wurtzite structure. Optimal bulk geometries have been calculated by total-energy minimzation. The Ga $3d$ and In $4d$ semicore electrons have been explicitly treated as valence electrons. For that reason and because of the lack of p electrons in the N and B cores ultrasoft non-normconserving pseudopotentials have been used in the plane-wave-pseudopotential code. We have demonstrated that the plane-wave cutoff can be reduced to values below 20 Ry. The resulting structural, lattice-dynamical, and polarization properties of the two polytypes of BN, AlN, GaN, and InN are rather close to the theoretical and experimental data available. Their trends with varying cation are clearly related to the different strengths of covalent and ionic bonding.

Considering heterocrystalline structures with large super-

cells including 30 group-III N bilayers, we have also calculated the spontaneous polarization field in the wurtzite structure. We observed an extreme sensitivity of the polarization on the equilibrium structure parameters. In addition, we have studied properties of the nitrides for displacements of the atoms from their equilibrium positions. The phonon frequencies are in excellent agreement with other data available in the literature. This holds also for the elastic stiffness constants that have been derived from the sound velocities. The *ab initio* calculations of phonons in InN have been presented. They allow a unique picture of the Raman modes in this material.

ACKNOWLEDGMENTS

We thank J. R. Leite for helpful discussions. This work was supported by the Deutsche Forschungsgemeinschaft (Sonderforschungsbereich 196 and Grant No. Be 1346/8-2).

[1] W.A. Harrison, *Electronic Structure and the Properties of Solids* (Dover, New York, 1989).
[2] A. Garcia and M.L. Cohen, Phys. Rev. B **47**, 4215 (1993).
[3] V.L. Solozhenko, in *Properties of Group III Nitrides*, edited by J.H. Edgar (INSPEC, London, 1994).
[4] S. Porowski and I. Grzegory, in *Properties of Group III Nitrides* (Ref. 3).
[5] I. Petrov, E. Mojab, R.C. Powell, J.E. Greene, L. Hultman, and J.-E. Sundgren, Appl. Phys. Lett. **60**, 1491 (1992); M.J. Paisley and R.F. Davis, J. Cryst. Growth **127**, 136 (1993).
[6] H. Harima, T. Inoue, S. Nakashima, H. Okumura, Y. Ishida, S. Yoshida, and H. Hamaguchi, J. Cryst. Growth **189/190**, 435 (1998).
[7] O. Brandt, H. Yang, B. Jenichen, Y. Suzuki, L. Däweritz, and K.H. Ploog, Phys. Rev. B **52**, R2253 (1995); D. Schikora, M. Hankeln, D.J. As, K. Lischka, A. Waag, T. Buhrow, and F. Henneberger, *ibid.* **54**, R8381 (1996).
[8] A.P. Lima, A. Tabata, J.R. Leite, S. Kaiser, D. Schikora, B. Schöttker, T. Frey, D.J. As, and K. Lischka, J. Cryst. Growth **201-202**, 396 (1999).
[9] K. Miwa and A. Fukumoto, Phys. Rev. B **48**, 7997 (1993).
[10] A.F. Wright and J.S. Nelson, Phys. Rev. B **60**, 2159 (1994); **51**, 7866 (1995).
[11] N.E. Christensen and I. Gorczyca, Phys. Rev. B **50**, 4397 (1994).
[12] G. Capellini, V. Fiorentini, K. Tenelsen, and F. Bechstedt, in *Gallium Nitride and Related Materials*, edited by R.D. Dupuis *et al.*, MRS Symposia Proceedings No. 395 (Materials Research Society, Pittsburgh, 1996), p. 429.
[13] K. Kim, W.R.L. Lambrecht, and B. Segall, Phys. Rev. B **53**, 16 310 (1996); **56**, 7018 (1997).
[14] D. Vogel, P. Krüger, and J. Pollmann, Phys. Rev. B **55**, 12 836 (1997).
[15] M. van Schilfgaarde, A. Sher, and A.B. Chen, J. Cryst. Growth **178**, 8 (1997).
[16] K. Karch and F. Bechstedt, Phys. Rev. B **56**, 7404 (1997).
[17] A. F. Wright, J. Appl. Phys. **82**, 2833 (1997).
[18] K. Karch, J.-M. Wagner, and F. Bechstedt, Phys. Rev. B **57**, 7043 (1998).
[19] C. Stampfl and C.G. van de Walle, Phys. Rev. B **59**, 5521 (1999).
[20] J. Furthmüller, P. Käckell, F. Bechstedt, and G. Kresse, Phys. Rev. B **61**, 4576 (2000).
[21] P. Hohenberg and W. Kohn, Phys. Rev. **136**, B864 (1964); W. Kohn and L.J. Sham, Phys. Rev. **164**, A1133 (1965).
[22] D. Vanderbilt, Phys. Rev. B **41**, 7892 (1990).
[23] U. Grossner, J. Furthmüller, and F. Bechstedt, Phys. Rev. B **58**, R1722 (1998).
[24] J.P. Perdew and A. Zunger, Phys. Rev. B **23**, 5048 (1981).
[25] D.J. Chadi and M.L. Cohen, Phys. Rev. B **8**, 5747 (1973).
[26] G. Kresse and J. Hafner, Phys. Rev. B **47**, R558 (1993).
[27] G. Kresse and J. Furthmüller, Comput. Mater. Sci. **6**, 15 (1996); Phys. Rev. B **54**, 11 169 (1996).
[28] F.D. Murnaghan, Proc. Natl. Acad. Sci. USA **30**, 244 (1944).
[29] P. Gianozzi, S. de Gironcoli, P. Pavone, and S. Baroni, Phys. Rev. B **43**, 7231 (1991).
[30] A. Dal Corso, A. Pasquarello, and A. Baldereschi, Phys. Rev. B **56**, R11 369 (1997).
[31] G. Kern, G. Kresse, and J. Hafner, Phys. Rev. B **59**, 8551 (1999).
[32] W. Frank, C. Elsässer, and M. Fähnle, Phys. Rev. Lett. **74**, 1791 (1995).
[33] G. Kresse, J. Furthmüller, and J. Hafner, Europhys. Lett. **32**, 729 (1995).
[34] W. Cochran and R. A. Cowley, J. Chem. Phys. Solids **23**, 447 (1962).
[35] G. L. Doll, in *Properties of Group-III Nitrides* (Ref. 3).
[36] H. Harima, T. Inoue, S. Nakashima, H. Okumura, Y. Ishida, S. Yoshida, T. Koizumi, H. Grille, and F. Bechstedt, Appl. Phys. Lett. **74**, 191 (1999).
[37] H. Siegle, G. Kaczmarczyk, L. Fillipidis, A.P. Litvinchuk, A. Hoffmann, and C. Thomson, Phys. Rev. B **55**, 7000 (1997).
[38] A. Tabata, R. Enderlein, J.R. Leite, S. W. da Silva, J.C. Galzerani, D. Schikora, M. Kloidt, and K. Lischka, J. Appl. Phys. **79**, 4137 (1996).
[39] P. Brüesch, *Phonons: Theory and Experiment I* (Springer-Verlag, Berlin, 1982), Chap. 4.
[40] M. Born and K. Huang, *Dynamic Theory of Crystal Lattices* (Clarendon, Oxford, 1954), Chap. 2.
[41] A. Tabata, A. P. Lima, L.K. Teles, L.M.R. Scolfaro, J.R. Leite, V. Lemos, B. Schüttker, T. Frey, D. Schikora, and K. Lischka, Appl. Phys. Lett. **74**, 362 (1999).
[42] M.-C. Lee, H.-C. Lin, Y.-C. Pan, C.-K. Shu, J. Ou, W.-H. Chen, and W.-K. Chen, Appl. Phys. Lett. **73**, 2606 (1998).
[43] H.-J. Kwon, Y.-H. Lee, O. Miki, H. Yamano, and A. Yoshida, Appl. Phys. Lett. **69**, 937 (1996).
[44] J. S. Dyck, K. Kash, K. Kim, W.R.L. Lambrecht, C.C. Hayman, A. Argoitia, M.T. Grossner, W.L. Zhou, and J.C. Angus, in *Nitride Semiconductors*, edited by F.A. Ponce *et al.*, MRS Symposia Proceedings No. 482 (Materials Research Society, Pittsburgh, 1998), p. 549.
[45] T. Inushina, A. Nagase, A. Iso, T. Yaguchi, and T. Shiraishi, *Proceedings of the 6th International Conference on Silicon Carbide and Related Materials* (Institute of Physics, London, 1996), p. 971.
[46] K. Osamura, S. Naka, and Y. Murakami, J. Appl. Phys. **46**, 3432 (1975).
[47] V.Yu. Davydov, V.V. Emtsev, I.N. Goncharuk, A.N. Smirnov, V.D. Petrikov, V.V. Mamutin, V.A. Vekshin, S.V. Ivanov, M.B.

Smirnov, and T. Inushima, Appl. Phys. Lett. **75**, 3297 (1999).
[48] M. Grimsditch, E. S. Zouboulis, and A. Polian, J. Appl. Phys. **76**, 832 (1994).
[49] V.Yu. Davidov, Yu.E. Kitaev, I.N. Goncharuk, A.N. Smirnov, J. Graul, O. Semchinova, D. Uffmann, M.B. Smirnov, A.P. Mirgorodsky, and R.A. Evarestov, Phys. Rev. B **58**, 12 899 (1998).
[50] E.T. Yu, G.J. Sullivan, P.M. Asbeck, C.D. Wang, D. Qino, and S.S. Lan, Appl. Phys. Lett. **71**, 2794 (1997).
[51] M. Leroux, N. Grandjean, M. Laügt, J. Massies, B. Gil, P. Lefebvre, and P. Bigenwald, Phys. Rev. B **58**, R13 371 (1998).
[52] R.M. Martin, Phys. Rev. B **9**, 1998 (1974).
[53] M. Posternak, A. Baldereschi, A. Catellani, and R. Resta, Phys. Rev. Lett. **64**, 1777 (1990).
[54] A. Qteish, V. Heine, and R.J. Needs, Phys. Rev. B **45**, 6534 (1992).
[55] F. Bechstedt and P. Käckell, Phys. Rev. Lett. **75**, 2180 (1995).
[56] F. Bechstedt, P. Käckell, A. Zywietz, K. Karch, B. Adolph, K. Tenelsen, and J. Furthmüller, Phys. Status Solidi B **202**, 35 (1997).
[57] F. Bernardini, V. Fiorentini, and D. Vanderbilt, Phys. Rev. B **56**, R10 024 (1997).
[58] F. Bernardini, V. Fiorentini, and D. Vanderbilt, Phys. Rev. Lett. **79**, 3958 (1997).